Supporting Information

Proton Probability Distribution in the O···H···O Low-Barrier Hydrogen Bond: A Combined Solid-State NMR and Quantum Chemical Computational Study of Dibenzoylmethane and Curcumin

Xianqi Kong,[a] Andreas Brinkmann,[b,] Victor Terskikh,[a,c] Roderick E. Wasylishen,[d,]* Guy M. Bernard,[d] Zhuang Duan,[d] Qichao Wu,[d] and Gang Wu[a,]**

[a]Department of Chemistry, Queen's University, 90 Bader Lane, Kingston, Ontario, K7L 3N6, Canada; [b]National Research Council Canada, 100 Sussex Drive, Ottawa, Ontario, K1A 0R6, Canada; [c]Department of Chemistry, University of Ottawa, 10 Marie Curie Private, Ottawa, Ontario, K1N 6N5, Canada; [d]Department of Chemistry, University of Alberta, Edmonton, Alberta, Canada T6G 2G2

*Corresponding authors:
E-mail: andreas.brinkmann@nrc-cnrc.gc.ca
E-mail: roderick.wasylishen@ualberta.ca
E-mail: gang.wu@chem.queensu.ca

Table S1. Comparison between experimental solid-state NMR ^{13}C isotropic chemical shifts and plane-wave DFT computational results[a] for dibenzoylmethane (**1**) and curcumin (**2**).

		δ_{iso} / ppm				
		Computational Model				
Molecule	Atom[b]	A	AB	B	<A+B>[c]	Expt.
dibenzoylmethane (**1**)	C1	183.0	187.9	191.7	187.3	188.0
	C2	94.9	94.1	93.6	94.2	92.9
	C3	190.9	187.8	183.3	187.1	182.7
	C4	134.9	133.8	132.7	133.8	133.0
	C5	130.4	129.6	128.7	129.5	127.9
	C6	129.8	129.8	129.9	129.9	127.9
	C7	132.9	133.0	132.9	132.9	131.9
	C8	130.9	131.3	131.5	131.2	129.0
	C9	127.9	127.7	127.6	127.8	126.7
	C10	136.4	137.5	138.7	137.5	135.9
	C11	128.4	128.6	128.8	128.6	126.7
	C12	130.5	130.5	130.5	130.5	129.0
	C13	134.6	135.0	135.3	134.9	133.0
	C14	131.2	131.4	131.6	131.4	129.7
	C15	129.4	129.8	130.2	129.8	127.9
curcumin (**2**)	C1	181.2	189.7	192.6	186.9	187.4
	C2	103.2	102.8	102.8	103.0	99.0
	C3	187.3	181.6	178.0	182.6	182.7
	C4	126.5	123.9	122.6	124.6	123.1
	C5	145.2	143.8	143.1	144.1	139.8
	C6	130.9	130.8	130.7	130.8	129.1
	C7	109.3	108.9	108.7	109.0	108.6
	C8	151.7	151.9	152.0	151.8	148.6
	C9	153.0	153.3	153.4	153.2	148.6
	C10	114.3	114.5	114.6	114.5	114.4
	C11	128.7	128.2	127.9	128.3	126.3
	C12	124.3	128.1	129.9	127.1	125.2
	C13	144.6	144.6	144.4	144.5	140.8
	C14	131.4	131.9	132.3	131.8	130.3
	C15	127.0	126.8	126.7	126.8	123.1
	C16	116.9	116.2	115.9	116.4	115.3
	C17	155.6	154.6	154.1	154.8	148.6
	C18	152.9	152.1	151.7	152.3	148.6
	C19	108.8	109.6	110.0	109.4	110.2
	C20	57.2	57.7	58.0	57.6	57.3
	C21	55.0	54.9	54.9	54.9	55.3

[a]To convert the computed ^{13}C magnetic shielding values into chemical shifts, σ_{ref} = 170.4 ppm was used; see also Figure S1; The uncertainties in experimental ^{13}C chemical shifts are ±0.1 ppm.
[b]See Scheme 2 in the main text for atomic labeling.
[c]Equal populations were assumed between Models A and B.

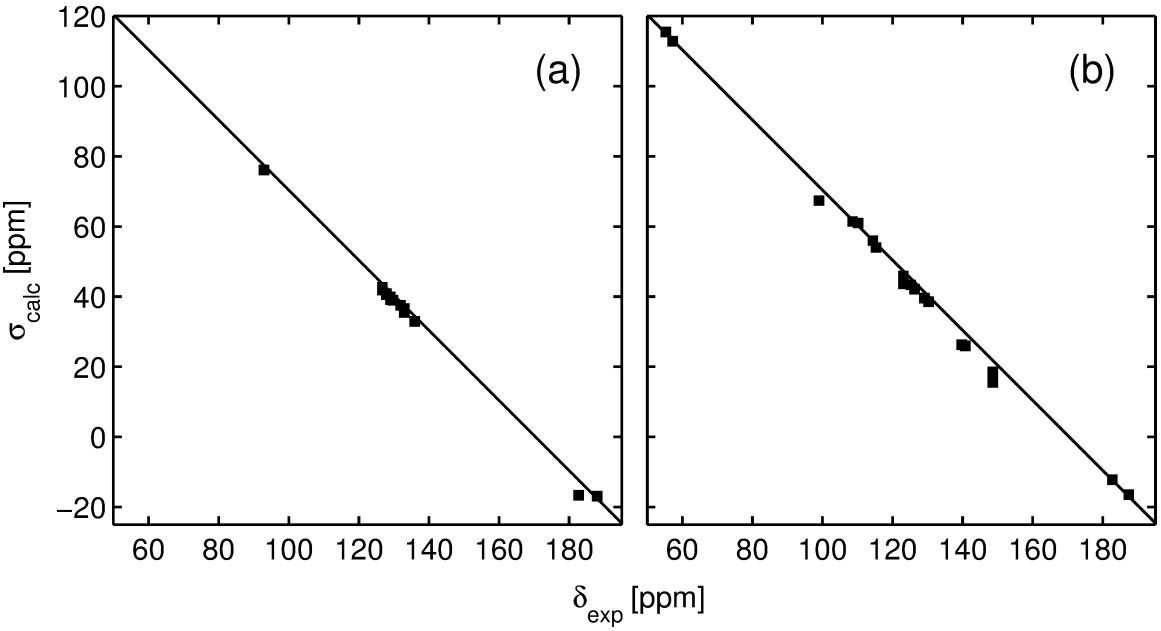

Figure S1. Squares: plane-wave DFT calculated values for the ^{13}C isotropic magnetic shielding constant, σ_{calc},for the computational model <A+B> with equal populations plotted against the experimental isotropic chemical shift δ_{exp} for **1** (a) and **2** (b). Solid-line: first order polynomial with the equation $\sigma_{calc} = -\delta_{exp} + 170.4$ ppm.

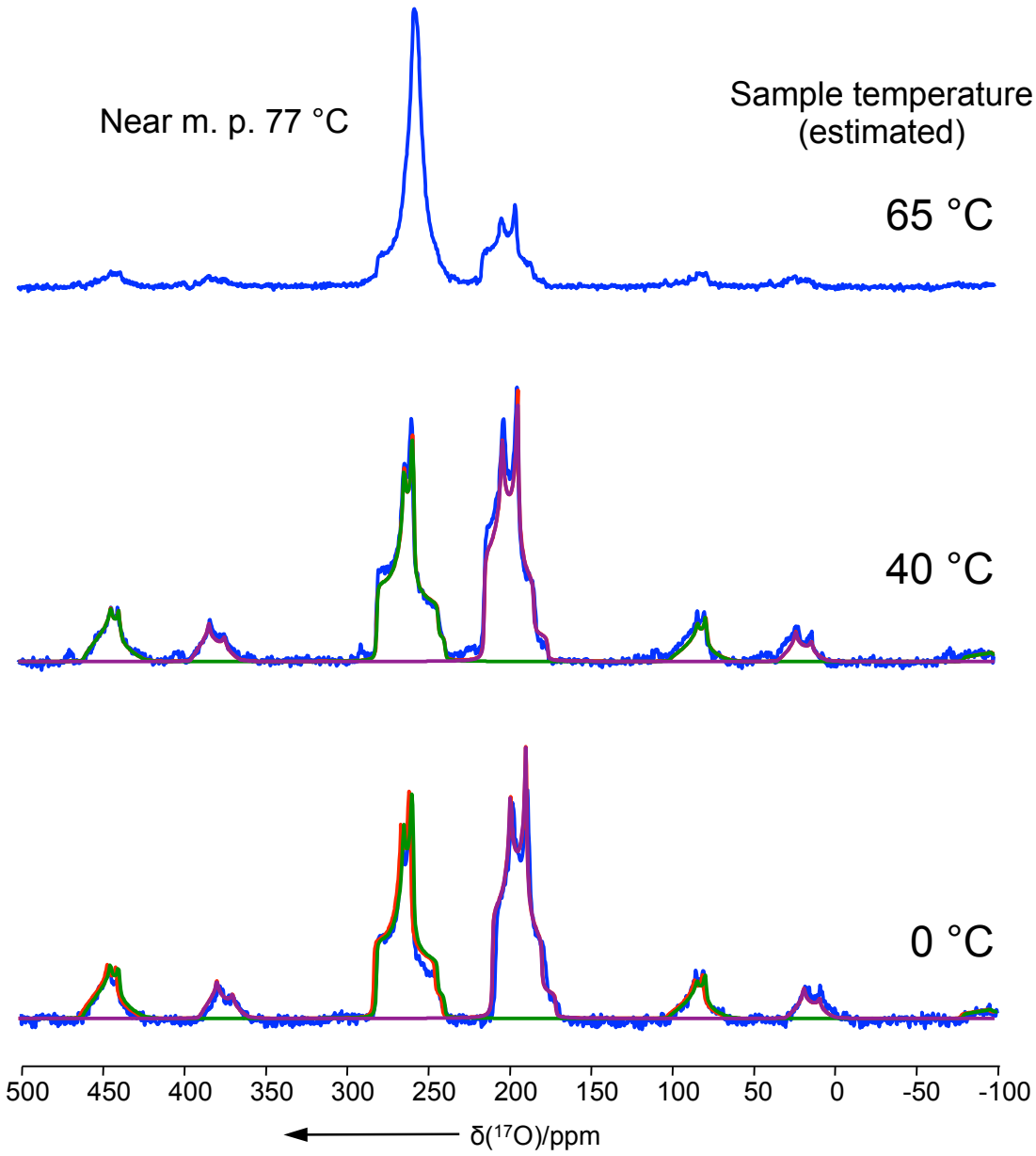

Figure S2. Variable-temperature ^{17}O MAS spectra of dibenzoylmethane (**1**) at 21.1 T.

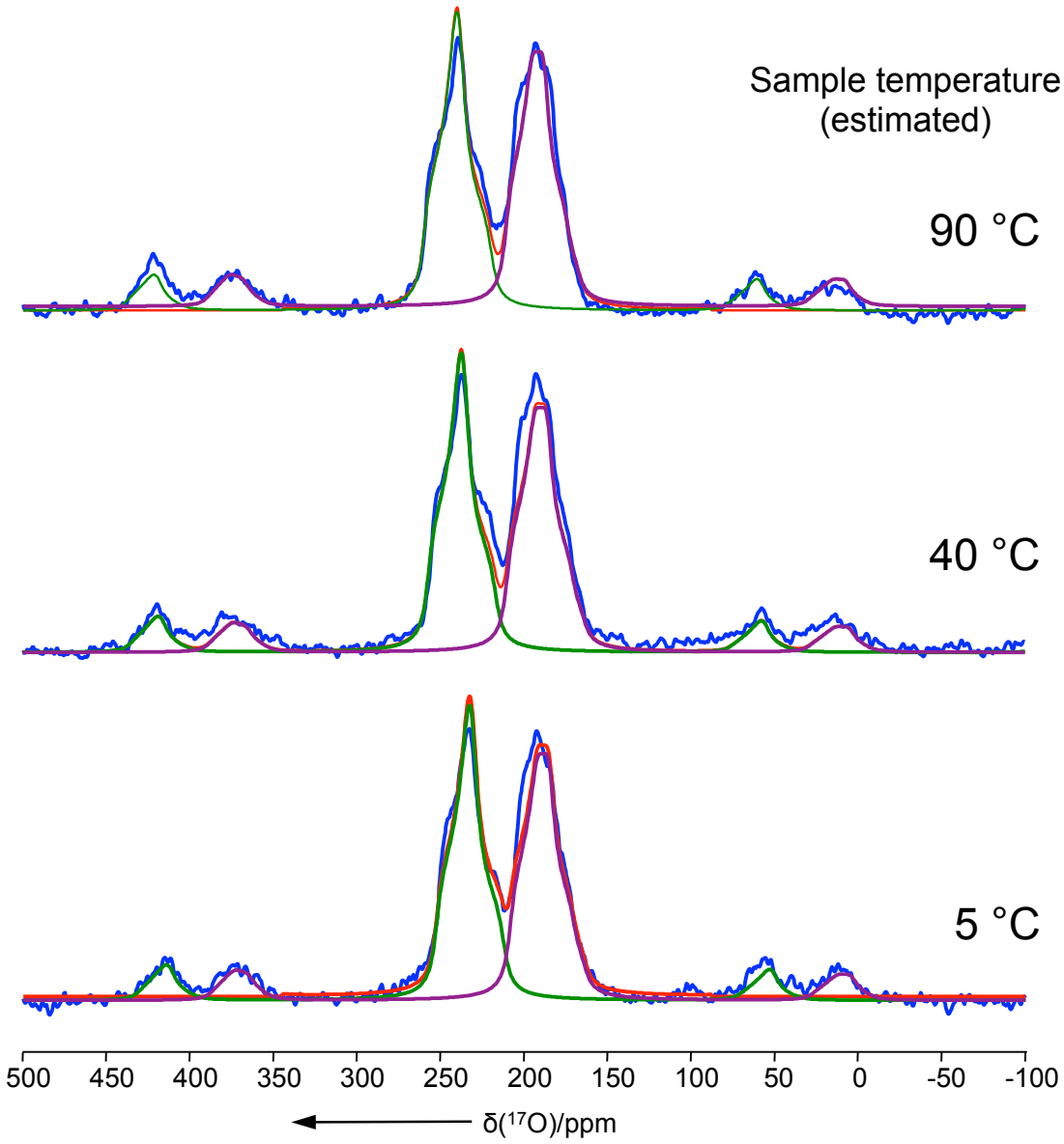

Figure S3. Variable-temperature ^{17}O MAS spectra of curcumin (**2**) at 21.1 T.